ELSEVIER

S100A9 regulates porcine reproductive and respiratory syndrome virus replication by interacting with the viral nucleocapsid protein

Zhongbao Song[a], Juan Bai[a], Xuewei Liu[a], Hans Nauwynck[b], Jiaqiang Wu[c], Xing Liu[d,**], Ping Jiang[a,e,*]

[a] *Key Laboratory of Animal Diseases Diagnostic and Immunology, Ministry of Agriculture, MOE International Joint Collaborative Research Laboratory for Animal Health & Food Safety, College of Veterinary Medicine, Nanjing Agricultural University, Nanjing 210095, China*
[b] *Laboratory of Virology, Faculty of Veterinary Medicine, Ghent University, Salisburylaan 133, B-9820 Merelbeke, Belgium*
[c] *Institute of Animal Husbandry and Veterinary Medicine, Shandong Academy of Agricultural Science, Jinan 250100, China*
[d] *Institute of Veterinary Medicine, Jiangsu Academy of Agricultural Sciences, Key Laboratory of Veterinary Biologicals Engineering and Technology, Ministry of Agriculture, National Center for Engineering Research of Veterinary Bio-products, Nanjing 210014, China*
[e] *Jiangsu Co-innovation Center for Prevention and Control of Important Animal Infectious Diseases and Zoonoses, Yangzhou, China*

ARTICLE INFO

ABSTRACT

Porcine reproductive and respiratory syndrome virus (PRRSV) has caused huge economic losses to the pig industry worldwide over the last 30 years, yet the associated viral-host interactions remain poorly understood. S100A9 is a damage-associated molecular pattern of the S100 protein family. Here, we found that PRRSV infection stimulated S100A9 expression in porcine alveolar macrophages (PAMs) and Marc-145 cells. S100A9 inhibited PRRSV replication via cellular Ca^{2+} dependent manner. The viral nucleocapsid (N) protein co-localized with S100A9 in the cytoplasm, and directly interacted at amino acid 78 of S100A9 and amino acids 36–37 of N protein. Moreover, we also found that the mutant S100A9 (E78Q) protein exhibited decreased antiviral activity against PRRSV compared with the parent S100A9. Recombinant PRRSV rBB (36/37) with two mutations in amino acid 36–37 in the N protein exhibited greater replication than the parent PRRSV BB0907 in S100A9-overexpressed PAM and Marc-145 cells. Thus, S100A9 may restrict PRRSV proliferation by interacting with the viral N protein.

1. Introduction

Porcine reproductive and respiratory syndrome virus (PRRSV) is the etiologic agent of porcine reproductive and respiratory syndrome (PRRS), commonly known as "blue ear disease." It is the main respiratory disease affecting swine and one of the costliest for the world's pork producers. PRRSV is a 15 kb single-stranded, positive-sense enveloped RNA virus, and its genome encodes 14 nonstructural (nsps) and eight structural proteins (Chen et al., 2017a,b; Li et al., 2007). Moreover, PRRSV infects pigs of all ages, causing fever, lethargy, inappetence, and respiratory distress (Jiang et al., 2000). The infection of pregnant sows often results in abortion, stillbirth, and mummified fetuses. Infected piglets often present with weakness, watery diarrhea, severe respiratory symptoms, and even death (Burkard et al., 2018). PRRSV was initially isolated in China in 1995, and the highly

pathogenic strain (HP-PRRSV) was isolated in China in 2006 (Tian et al., 2007), and it has since spread widely, taking a large economic toll on China's pork producers. The main clinical symptoms of HP-PRRSV include high fever, dyspnea, and rubefaction, whereas the primary pathological symptom is interstitial pneumonia (Li et al., 2007; Tian et al., 2007). Since 2012, NADC30-like strains have become more prevalent in China, increasing the difficulty of prevention and control (Li et al., 2016; Wang et al., 2017a, b).

The innate immune response is the host's first line of defense against pathogen invasion. In general, interferons (IFNs) are one of the earliest cytokines produced following viral invasion. Initially, host pattern recognition receptors (PRRs) recognize pathogens and activate I type IFN signaling via IRF3 and NF-κB to produce multiple interferon-stimulated proteins to inhibit viral infection (Wuerth et al., 2018). However, as an immunosuppressive virus, PRRSV has many immunosuppressive

---

mechanisms of inhibiting the host innate and adaptive immune responses to support viral replication (Chen et al., 2018). PRRSV nsp1α inhibits IFN-β production by degrading CREB-binding protein (CBP) and suppressing NF-κB activation (Kim et al., 2010). In addition, nsp1β and nsp2 can hinder the activation of IRF3 to inhibit IFN-β expression (Beura et al., 2010; Li et al., 2010). NF-κB-essential modulator (NEMO) is an essential molecule for NF-κB activation, and MAVS is an upstream molecule in the IFN-β pathway; PPRSV nsp4 can cleave these two molecules to decrease IFN-β production (Huang et al., 2016; Huang et al., 2014). Moreover, PRRSV infection can induce the apoptosis DC cells (Huang et al., 2015), reduce the expression of antigen presenting molecules on the surface of antigen presenting cells (Chen et al., 2018), inhibit the proliferation and differentiation of B and T cells (Loving et al., 2015), and promote the production of immunosuppressive cells (e.g., regulatory T cells) (Fan et al., 2015). In addition, the rapid mutation and recombination of PRRSV are associated with a substantial challenge to both viral prevention and control. Although there are several commercially available vaccines, their effectiveness is limited. Therefore, it is extremely important to study the pathogenesis of PRRSV further, which remains poorly understood.

PRRSV nucleocapsid protein is a multifunctional protein that is essential for viral replication. Thus, N protein is likely to be the target of host innate immune molecules for inhibiting viral propagation. Jing et al. (2019) indicated that TRIM22 can reduce PRRSV replication through interacting with N protein nuclear localization signal (NLS). And MOV10 could co-localize with the PRRSV N protein in the cytoplasm and disturb the distribution of N protein in the cells, leading to the retention of N protein in the cytoplasm (Zhao et al., 2018). In addition, Wang et al. (2017a, b) reported that SUMO E2 conjugating enzyme Ubc9 can interact with and SUMOylate N protein to regulate PRRSV replication.

Damage-associated molecular patterns (DAMPs) are biomolecules that can activate the innate immune response, as well as directly or indirectly initiate the adaptive immune response (Pouwels et al., 2014). Numerous DAMPs have been identified, including high mobility group box 1 (HMGB1), heat shock proteins (HSPs), and S100 proteins. These DAMPs may participate in viral replication, to some extent, using a variety of different means (Liu et al., 2013, 2016; Trinh et al., 2016). S100 calcium-binding protein A9 (S100A9) is a member of the S100 family of calcium-binding proteins. A recent study showed that S100A9 is a host restrictive factor that possesses antiviral activity against bovine viral diarrhea virus (BVDV) replication (Darweesh et al., 2018). In our previous proteomics study, we found that the expression of S100A9 was significantly increased in PRRSV-infected PAMs (data not shown); however, the role of S100A9 in PRRSV infection remains unknown. In this study, we report that S100A9 has significant antiviral activity against PRRSV replication, and interacts with the viral N protein at amino acid 78 of S100A9 and amino acids 36–37 of the viral N protein, respectively. These findings suggest a novel host antiviral mechanism against PRRSV.

2. Materials and methods

2.1. Cells and virus

Marc-145 cells, a monkey embryonic kidney cell line that is highly permissive for PRRSV, and HEK293T cells were cultured in Dulbecco's Modified Eagle's Medium (DMEM) (Invitrogen, Carlsbad, CA, USA) supplemented with 10 % heat-inactivated fetal bovine serum (FBS) (Gibco, Grand Island, NY, USA), 100 U/mL penicillin, and 100 μg/mL streptomycin. The cells were incubated at 37 °C in a humidified atmosphere containing 5 % CO_2. Porcine alveolar macrophages (PAMs) were obtained from five-week-old piglets, which were free of PRRSV, pseudorabies virus, porcine circovirus type 2, and classical swine fever virus. Moreover, the PAMs were maintained in Roswell Park Memorial Institute 1640 medium (RPMI 1640) (Invitrogen) containing 10 % FBS,

1 % non-essential amino acids (Invitrogen), 100 U/mL penicillin, and 100 μg/mL streptomycin. The cells were incubated in a 37 °C humidified atmosphere containing 5 % CO_2. The classical PRRSV S1 strain (C-PRRSV) (GenBank accession No. AF090173) was obtained from clinical material in Jiangsu province in 1997. The BB0907 strain (GenBank accession No. HQ315835) is a highly pathogenic strain of PRRSV (HP-PRRSV) that was isolated from clinical samples collected in Guangxi province, China, in 2009. The NADC30-like PRRSV strain, FJ1402 (GenBank accession No. KX169191.1), was isolated from clinical materials in Fujian province, China, in 2014. Recombinant virus rBB (36/37) was rescued from the infectious clone, pCMV-BB0907 (constructed in our laboratory), as previously described (Liu et al., 2015b). The viruses were cultured and tittered in Marc-145 cells.

2.2. Antibodies and reagents

Anti-HA, FLAG, and β-actin mouse monoclonal antibodies were purchased from Proteintech (USA, Chicago), and an anti-S100A9 rabbit polyclonal antibody was purchased from Abcam (Cambridge, UK). BAPTA, a specific intracellular Ca^{2+} chelating agent, was purchased from MedChemExpress (New Jersey, USA). PMSF was purchased from Solarbio (Beijing, China). The anti-PRRSV N protein mAb was prepared in our lab.

2.3. Plasmids and siRNA

Total RNA was extracted from Marc-145 cells or PAMs, and used for cDNA synthesis. *S100A9* was amplified via PCR and cloned into the pCI-neo vector with a 3′ HA tag. Sequence verification of the resulting plasmid, pCI-S100A9-HA, was conducted by Genscript Biotechnology Co., Ltd. (Nanjing, China). The nucleotide sequence of *S100A9* was found to have a 98.2 % similarity to that in NCBI using DNAStar 8.0 software.

PRRSV genes were amplified from the BB0907 strain by PCR and cloned into the pCI-neo vector with a 3′ FLAG tag. Following the sequence verification of the resulting plasmids, all of the recombinant plasmids were transfected into HEK293T cells to verify that these proteins were efficiently expressed. However only Nsp1α, Nsp1β, Nsp4, Nsp5, Nsp7, Nsp9-12, GP5, M, and N proteins could be efficiently expressed (data not shown). Plasmids expressing the mutated PRRSV N protein, pCI-N*-FLAG, were previously constructed in our lab (Liu et al., 2015b). Fig. S1 presents a diagram of these mutated plasmids.

According to the key amino acid of human S100A9 reported at https://www.uniprot.org/, a series of mutated S100A9 plasmids were constructed. These constructs were created using a QuikChange® II XL Site-Directed Mutagenesis Kit (Stratagene, La Jolla, CA, USA) according to the manufacturer's instructions. All plasmids were efficiently expressed in 293T cells.

Three pairs of specific siRNAs for monkey or porcine *S100A9* and a non-specific control siRNA were designed by GenePharma (Shanghai, China). Macr-145 or PAM cells were transfected with siRNAs using Lipofectamine™ RNAiMAX Transfection Reagent (Invitrogen) according to the manufacturer's instructions. The siRNA sequences of monkey or porcine S100A9 used in this study are as follows, siRNA1, 5′-GAACCG GAGGGAAUUCAAATT-3′; siRNA2, 5′-GCAGCU GGAACGCAACAU ATT-3′; siRNA3, 5′-GGACACAAAUGCAGACAAGTT-3′; and siRNA-1, 5′-GCAGAUGGAAUGCAGCAUATT-3′; siRNA-2, 5′-GCUGCCAAACUUU CUCAAGTT-3′; siRNA-3, 5′-CGA AAUAAAGUCUCCCUCUTT-3′.

2.4. Lentivirus packaging

S100A9 and *S100A9 (E78Q)* were cloned into the lentiviral expression plasmid, pCDH-CMV-MCS-EF1-GFP-Puro, (kindly provided by Professor HeBin, Illinois State University, USA), to generate recombinant plasmids. A recombinant plasmid and two packaging plasmids, psPAX2 and PMD2.G, were co-transfected into HEK293T cells at a

ratio of 4:3:1, and the supernatants were collected at 48 h and 60 h after transfection, respectively. Viral supernatants were concentrated using a lentivirus concentration kit (Genomeditech Biotech Co., Ltd., Shanghai, China) according to the manufacturer's instructions. Viral titers were measured in HEK293T cells.

2.5. Western blotting analyses

The cells were harvested using RIPA buffer containing PMSF. Samples were centrifuged at $12,000 \times g$ for 5 min to remove the insoluble material. Supernatants were collected and their total protein concentration was measured using a BCA kit. Equal amounts of protein with $5 \times$ loading buffer were placed into a boiling water bath for 5 min and then loaded into the wells of a 10 % SDS-polyacrylamide gel, after which the separated proteins were transferred onto a nitrocellulose membrane. The membranes were blocked with 10 % nonfat milk for 2 h at room temperature (RT), and then incubated with primary antibodies for 2 h at RT. After washing, the membranes were incubated with a secondary antibody for 1 h at RT. The membranes were rinsed once again, and images were captured using Thermo Pierce ECL substrate with a Tanon5200 Chemi-Image system (Biotanon, Shanghai, China).

2.6. Quantitative real-time PCR

Total RNA Kit I (Omega Bio-tek, Shenzhen, China) was used to extract RNA from cells and synthesize the cDNA. qPCR was performed in an ABI QuantStudio 6 Systems (Applied Biosystems, Foster City, CA, USA) using a SYBR-Green RT-PCR Master Mix (Applied Biosystems). The PCR conditions were as follows: an initial denaturation for 5 min at 95 °C, followed by 40 cycles of 15 s at 95 °C, and 1 min at 60 °C. All of the primer sequences that were used are as follows, monkey *S100A9,* 5′-GCTGGAACGCAACATAGAGA-3′ and 5′-CTGGTT CAGGGTGTCTT TGT-3′; porcine *S100A9,* 5′-CAACATCTTCCACCAGTACTCG-3′ and 5′-CATT AGTGTCCAGGTCTTCCAG-3′; PRRSV N gene, 5′-AAACCAGTCC AGAGGCAAGG-3′ and 5′-TCAGTCGCAAGAGGGAAATG-3′; β-anctin, 5′-CTCCATCATGAAGTGCGACGT-3′ and 5′-GTGATCTCCTTCTGCATCC TGTC-3′. Duplicate samples of each transcript were analyzed, and the level of expression for all genes was normalized to that of β-actin. The results were calculated using the $2^{-\Delta\Delta CT}$ method.

2.7. Immunofluorescence assay

Virus-infected and plasmid-transfected cells were fixed with 10 % formalin-PBS for 10–15 min at RT, rinsed with PBS, then permeabilized with prechilled acetone (-20 °C) for exactly 5 min. Cells were rinsed again and blocked with 1 % BSA-PBS for 1 h at RT. Cells were incubated with primary antibodies for 1 h at 37 °C, then washed three times with PBS, followed by an incubation with a fluorescence-labeled secondary antibody for 1 h at 37 °C. The cells were rinsed again, and the nuclei were stained with DAPI for 10 min at RT. Cells were observed using a confocal laser-scanning microscope (Zeiss LSM 510 system, Carl Zeiss AG, Oberkochen, Germany).

2.8. Immunoprecipitation

HEK293 T cells were seeded into six-well plates and cultured overnight, and the cells were co-transfected with pCI-S100A9-HA and pCI-*N*-FLAG or pCI-N*-FLAG. At 24 h post-transfection, the cells were washed three times with PBS and then incubated with RIPA buffer for 10–15 min on ice. The cell lysates were collected and centrifuged at $10,000 \times g$ for 10 min at 4 °C. Supernatants were transferred to fresh tubes on ice, and 1 μg of mouse IgG and 20 μL of protein A/G agarose (Santa Cruz Biotechnology, Texas, USA) were added to each tube. After incubation for 1 h at 4 °C, the samples were centrifuged at $1000 \times g$ for 5 min at 4 °C to remove any beads. The supernatants were collected and an anti-HA (1:1000) antibody was added to each tube. After an

incubation for 1 h at 4 °C, 20 μL protein A/G agarose was added to each sample and the incubation continued at 4 °C overnight. The immunoprecipitated proteins were collected by centrifugation at $1000 \times g$ for 5 min at 4 °C. After washing three times in RIPA buffer, the immunoprecipitated proteins were resuspended in 100 μL RIPA for western blot analysis.

2.9. Ethics statement

All animal experiments were performed in accordance to the guidelines of the Institutional Animal Care and Ethics Committee of Nanjing Agricultural University (NAU) (Nanjing, Jiangsu, China). All animals were raised in the NAU animal facility, and all operations were performed in accordance with the International Guiding Principles for Biomedical Research Involving Animals.

2.10. Statistical analyses

The significance of the variability among groups was analyzed with GraphPad Prism 7.0 software (GraphPad, La Jolla, CA, USA) using a one-way analysis of variance or a Student's unpaired two-tailed test. Differences were considered to be statistically significant if $P < 0.05$. Densitometric analyses were performed using Quantity One 4.6 software (Bio-Rad, Hercules, CA, USA).

3. Results

3.1. PRRSV infection stimulates S100A9 expression in PAMs and Marc-145 cells

PAMs were infected with PRRSV at various multiplicities of infection (MOI) for 24 h; qRT-PCR was performed to quantitate the level of S100A9 mRNA and viral N protein gene expression. The results showed that the level of S100A9 mRNA was upregulated by PRRSV in a dose-dependent manner (Fig. 1A).

MARC-145 cells were infected with PRRSV (0.1 MOI) for 12 h, 24 h, 36 h, and 48 h. Then a Western blot and qRT-PCR were used to determine the effect of PRRSV infection on S100A9 expression in Marc-145 cells. The results revealed that PRRSV infection significantly promoted both the level of S100A9 mRNA and protein expression from 24 to 48 hpi (Fig. 1B and C). These results indicated that PRRSV infection promotes S100A9 expression.

3.2. S100A9 inhibits PRRSV replication

To explore whether S100A9 affects the replication of PRRSV, Marc-145 cells were transfected with pCI-S100A9-HA for 24 h, then incubated with 0.01 MOI PRRSV for 12 h, 24 h, and 36 h. A western blot and qRT-PCR assay analysis showed that the level of PRRSV N protein was significantly decreased in cells overexpressing S100A9 compared with those in the empty vector-transfected cells at all-time points (Fig. 2A, and C). TCID$_{50}$ assay also showed that PRRSV titers were obviously decreased in cells overexpressing S100A9 (Fig. 2B).

The silencing efficiency of three siRNAs targeting monkey *S100A9* was tested in Marc-145 cells and examined by western blot. As shown in Fig. 2D, siRNA3 was the most efficient at decreasing the expression of endogenous S100A9. Then Marc-145 cells transfected with 50 nM siRNA3 and subsequently infected with PRRSV (0.01 MOI) exhibited greater expression of PRRSV N protein compared with the cells transfected with the negative siRNA control (NC) (Fig. 2E). Moreover, the qRT-PCR and TCID$_{50}$ data also revealed that the knockdown of S100A9 was beneficial for viral proliferation (Fig. 2F and G). In addition, S100A9 overexpression inhibited the proliferation of classical PRRSV strain (C-PRRSV), S1, and the epidemic NADC30-like strain, FJ1402 (Fig. 2H–J).
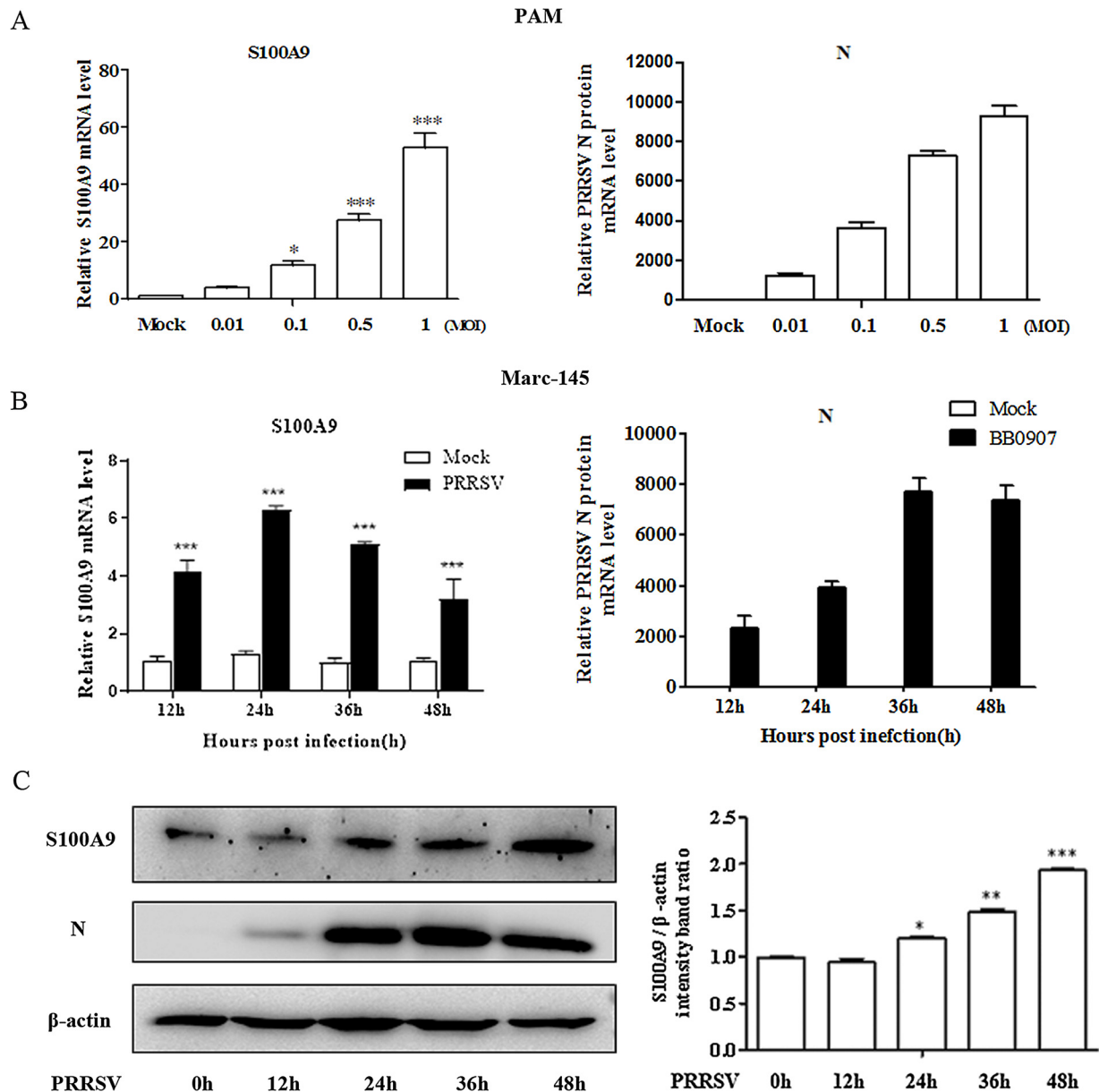
Fig. 1. PRRSV infection induces S100A9 in PAM and Marc-145 cells. (A) PAMs were infected with the PRRSV BB0907 strain for 24 h. qRT-PCR was used to quantitate the level of S100A9 and N protein mRNA expression. (B) Marc-145 cells were infected with 0.1 MOI of the BB0907 strain for 12 h, 24 h, 36 h, and 48 h. The qRT-PCR was used to quantitate the level of S100A9 and N protein mRNA expression. (C) Western blot analysis was used to determine the level of S100A9 and N protein expression. All of the results are expressed as the means + standard deviation from three independent experiments.

3.3. S100A9 inhibition of PRRSV replication is dependent on intracellular Ca^{2+}

Because S100A9 contains two EF hand calcium-binding domains, we hypothesized that calcium could affect the antiviral activity of S100A9. Firstly, the cytotoxicity of BAPTA was tested. The result showed that BAPTA, at concentration as high as 80 μM for 48 h, did not show cytotoxicity toward Marc-145 cells (Fig. 3A), as determined by Cell Counting Kit-8. Then Marc-145 cells were transfected with pCI-S100A9-HA, subsequently treated with BAPTA for 24 h, and infected with PRRSV for another 36 h. The cells treated with BAPTA had significantly higher levels of PRRSV N-protein expression in a dose dependent manner compared to untreated cells, as shown by western blot and qRT-PCR (Fig. 3B and C). Additionally, a TCID$_{50}$ assay showed that chelating intracellular Ca^{2+} resulted in increased PRRSV proliferation in infected cells overexpressing S100A9 (Fig. 3D). This finding demonstrated that the activity of S100A9 against PRRSV propagation was

dependent on intracellular Ca^{2+}.

3.4. S100A9 interacts with the PRRSV N protein

To screen for viral proteins that interact with S100A9, HEK293 T cells were co-transfected with pCI-S100A9-HA and recombinant plasmids expressing PRRSV Nsp1α, Nsp1β, Nsp4, Nsp5, Nsp7, Nsp9-12, GP5, M, and N protein genes. The Co-IP results showed that S100A9 efficiently co-precipitated with only the N protein (Fig. 4A and B). To visualize the interaction between S100A9 and the N protein, Marc-145 cells were transfected with pCI-S100A9-HA for 24 h, then infected with PRRSV at an MOI of 0.1 36 hpi. Confocal microscopy showed the co-localization of S100A9 (red) and N protein (green) in the cytoplasm. Infection with PRRSV did not alter the distribution of S100A9 (Fig. 4C).
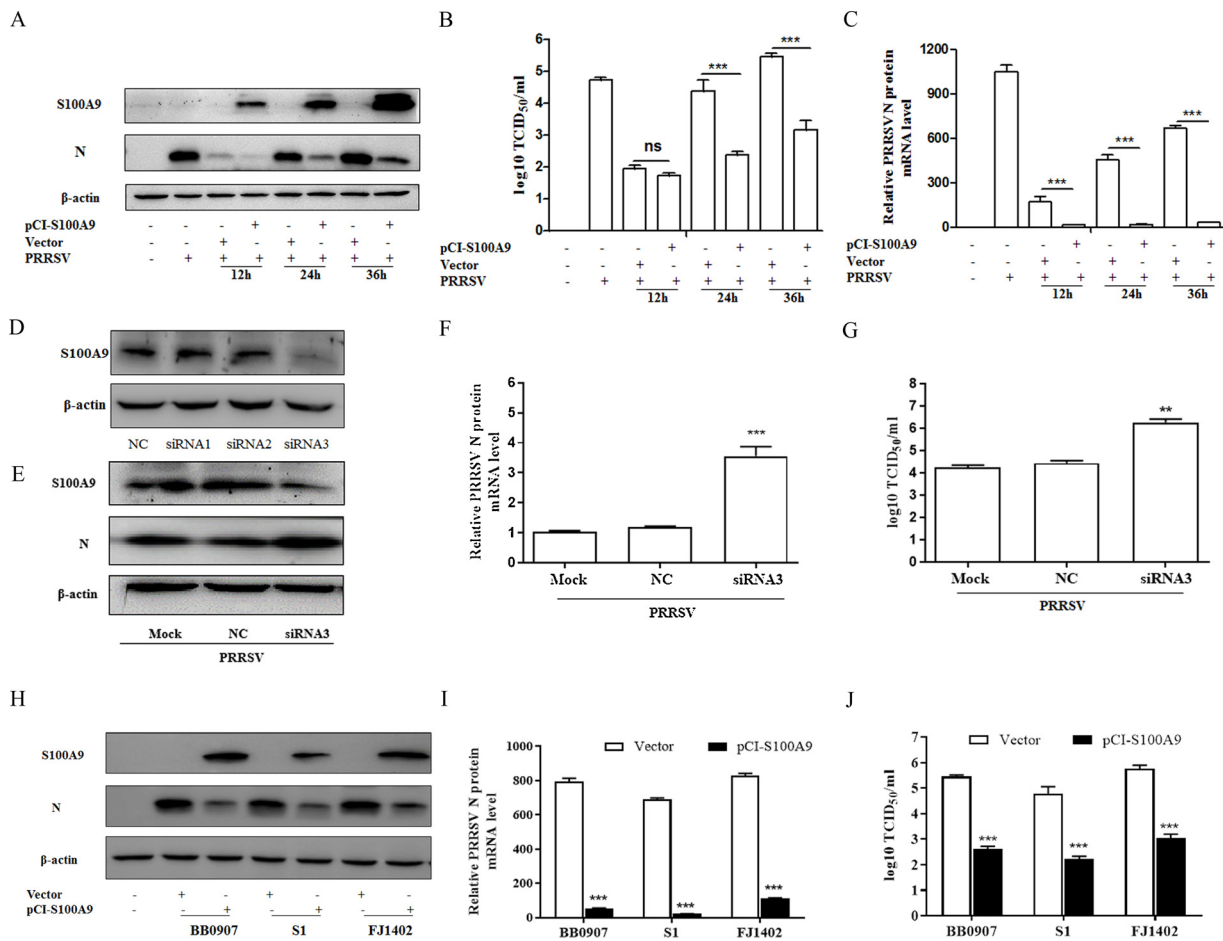
Fig. 2. S100A9 inhibits PRRSV replication. (A) Western blot assay for N protein of Marc-145 cells transfected with pCI-S100A9-HA or an empty vector for 24 h, and then infected with the PRRSV BB0907 strain (0.01 MOI), for 24 h, 36 h, and 48 h. (B) The level of N protein mRNA expression by qPCR and (C) PRRSV titer by TCID$_{50}$ assay. (D) Western blot of Marc-145 cells transfected with three siRNAs targeting monkey *S100A9*. (E—G) Western blot, qRT-PCR, and TCID$_{50}$ of Marc-145 cells transfected with siRNA3 for 24 h, then infected with the PRRSV BB0907 strain for 36 h. (H—J) Western blot, qRT-PCR, and TCID$_{50}$ of Marc-145 cells transfected with pCI-S100A9-HA or control vector for 24 h, then infected with the PRRSV strains BB0907, S1, and FJ1402 for 36 h. All results are expressed as the means + standard deviations from three independent experiments.

3.5. The key amino acids of the PRRSV N protein are required for the interaction with S100A9

To determine the region of the N protein that interacts with S100A9, a series of plasmids expressing a mutant N protein were co-transfected with pCI-S100A9-HA. Co-IPs were performed, and the results showed that S100A9 co-precipitated with all of the mutated N proteins except for Q33-5A (Fig. 5A-C), indicating that the S100A9 interacting region of the viral N protein is located at amino acids 33–37. Five plasmids expressing separate point mutations within this region of the N protein were constructed. Co-IP analysis showed that S100A9 efficiently co-precipitated with the mutations Q33A, N34A, and Q35A, but not S36A and R37A (Fig. 5D), which demonstrated that S36 and R37 are the key amino acids necessary for the interaction between the viral N protein and S100A9.

To confirm the role of S36 and R37 in the viral N protein, a recombinant virus, rBB (36/37), was constructed and rescued from the infectious clone, pCMV-BB0907, as previously described (Fig. S2) (Liu et al., 2015a). The growth kinetics of rBB (36/37) in Marc-145 cells was similar to that of the parent strain, BB0907 (Fig. 5E). The antiviral activity of S100A9 against the recombinant virus, rBB (36/37), was significantly decreased compared with that against the parent BB0907 as determined by western blot, qPCR, and TCID$_{50}$ assay (Fig. 5F-H).

3.6. The key amino acids of S100A9 are necessary for its interaction with the PRRSV N protein

To investigate the S100A9 amino acids that affect PRRSV replication, a series of plasmids expressing mutations in S100A9 were constructed and co-transfected with pCI-N into HEK293 T cells. The Co-IP results showed that only the mutant E78Q did not co-precipitate with the N protein, demonstrating that E78 is the key amino acid involved in the interaction between S100A9 and PRRSV (Fig. 6A). Thereafter, Marc-145 cells were transfected with plasmids expressing mutated S100A9 for 24 h, then infected with PRRSV at an MOI of 0.01. As shown in Fig. 6B and C, S100A9 with the E78Q mutation displayed significantly less antiviral activity than wild type S100A9. These results demonstrated that E78 was an amino acid required for the anti-PRRSV activity of S100A9.

3.7. S100A9 inhibits PRRSV replication in PAMs

Porcine alveolar macrophages (PAMs) are the target cells of PRRSV. To investigate the effect of S100A9 on PRRSV replication in PAMs, three siRNAs targeting porcine S100A9 were designed. As shown in Fig. 7A, siRNA-3 was found to be the most effective at silencing the expression of endogenous S100A9, reducing it by 50 %. A transfection with siRNA-3 significantly enhanced PRRSV replication compared with that of the control siRNA (Fig. 7B and C). Next, two recombinant
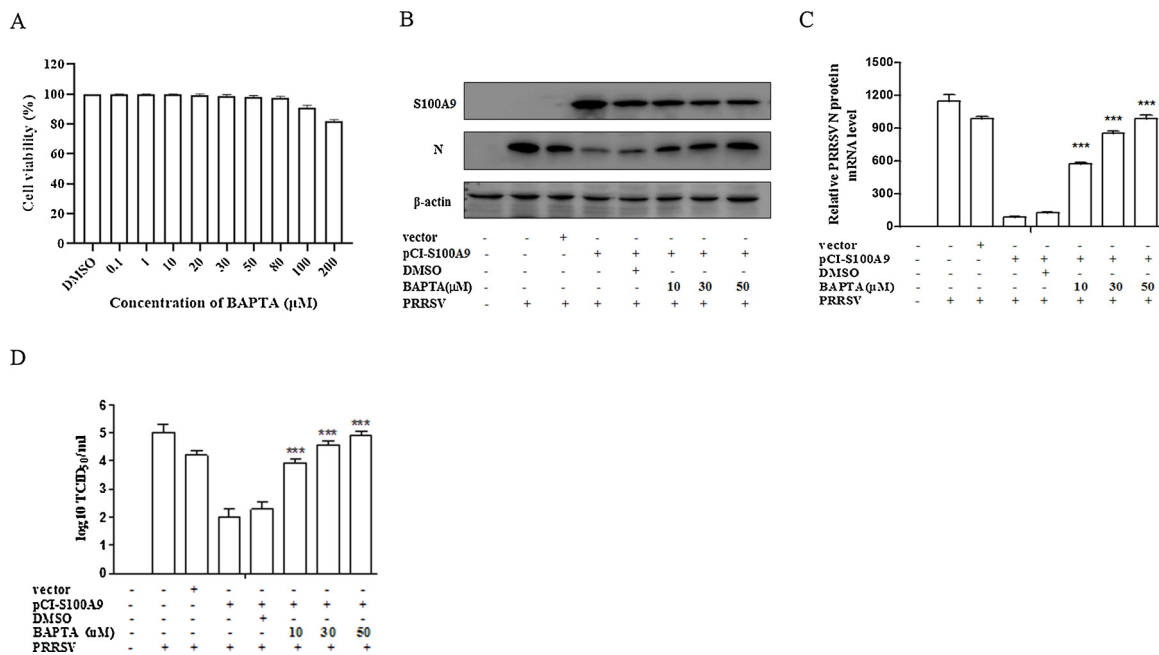
Fig. 3. S100A9 inhibition of PRRSV replication is dependent on intracellular Ca^{2+}. Marc-145 cells were transfected with pCI-S100A9-HA for 6 h, then treated with BAPTA (10 μM, 30 μM, and 50 μM), and infected with PRRSV an MOI of 0.01 for 36 h. Cells were lysed and analyzed by (A) western blot, (B) real time PCR, and (C) TCID$_{50}$ assay. All the results were confirmed by three independent experiments. Error bars represent the standard deviations of triplicate experiments.

lentiviruses, LV-S100A9 and LV-S100A9(E78Q), expressing S100A9 and S100A9(E78Q), respectively, were constructed and rescued. PAMs were transduced with recombinant lentiviruses at an MOI of 10 following infection with PRRSV BB0907 or rBB(36/37) at an MOI of 0.01. These results showed that PRRSV BB0907 strain replication was significantly restricted in LV-S100A9-transduced PAMs, whereas PRRSV rBB(36/37) replication was not (Fig. 7D and E).

Additionally, the replication of the BB0907 strain was significantly limited in both LV-S100A9 and LV-S100A9(E78Q)-transduced PAMs. However, the level of viral replication in LV-S100A9(E78Q)-transduced cells was notably reversely increased compared to those in LV-S100A9 transduced cells, as demonstrated by western blot and qRT-PCR assays (Fig.7F and G). These results demonstrated that S100A9 inhibited PRRSV replication in PAMs. In addition, the E78 in S100A9 played an
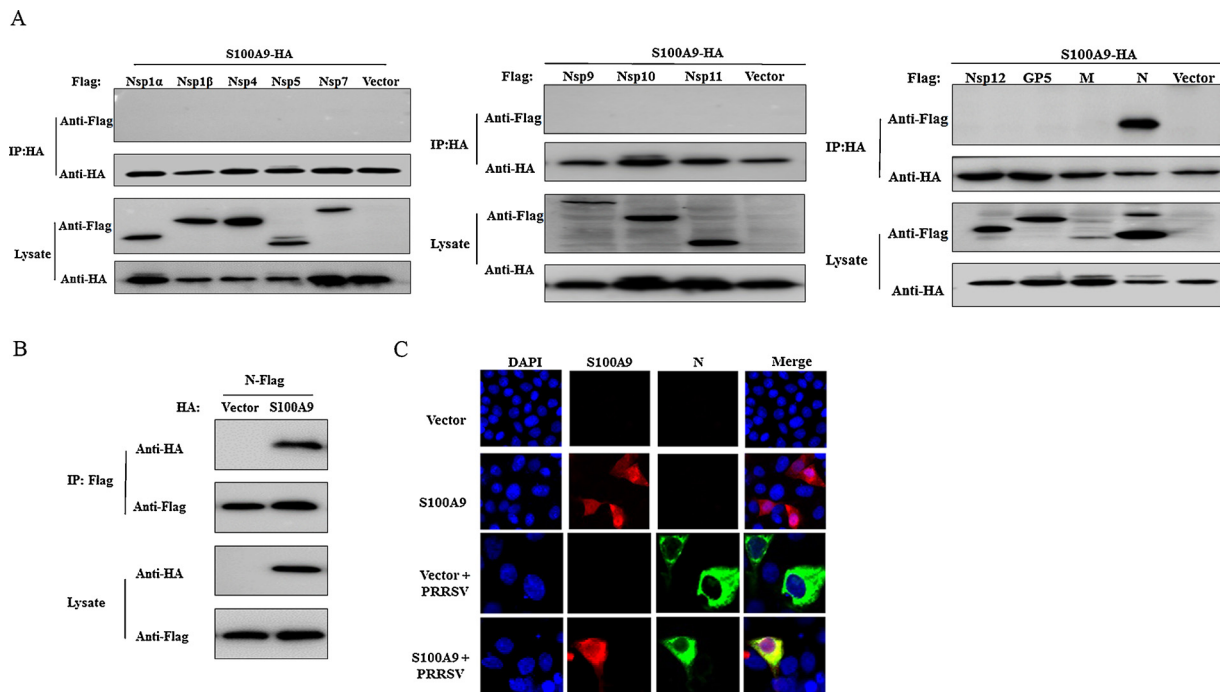

Fig. 4. S100A9 interacts with the PRRSV N protein. HEK293T cells were co-transfected with pCI-S100A9-HA and plasmids encoding PRRSV proteins (nsp1α, nsp1β, nsp4, nsp5, nsp7, nsp9-12, GP5, M, and N) for 30 h then prepared for immunoprecipitation by (A) an anti-FLAG antibody or (B) anti-HA antibody. (C) Immunofluorescence assay of Marc-145 cells transfected with pCI-S100A9-HA or vector for 24 h, then infected with PRRSV for 30 h. The S100A9 (red) N protein (green) and nuclei (blue). All the results were confirmed by three independent experiments. (For interpretation of the references to colour in this figure legend, the reader is referred to the web version of this article.)
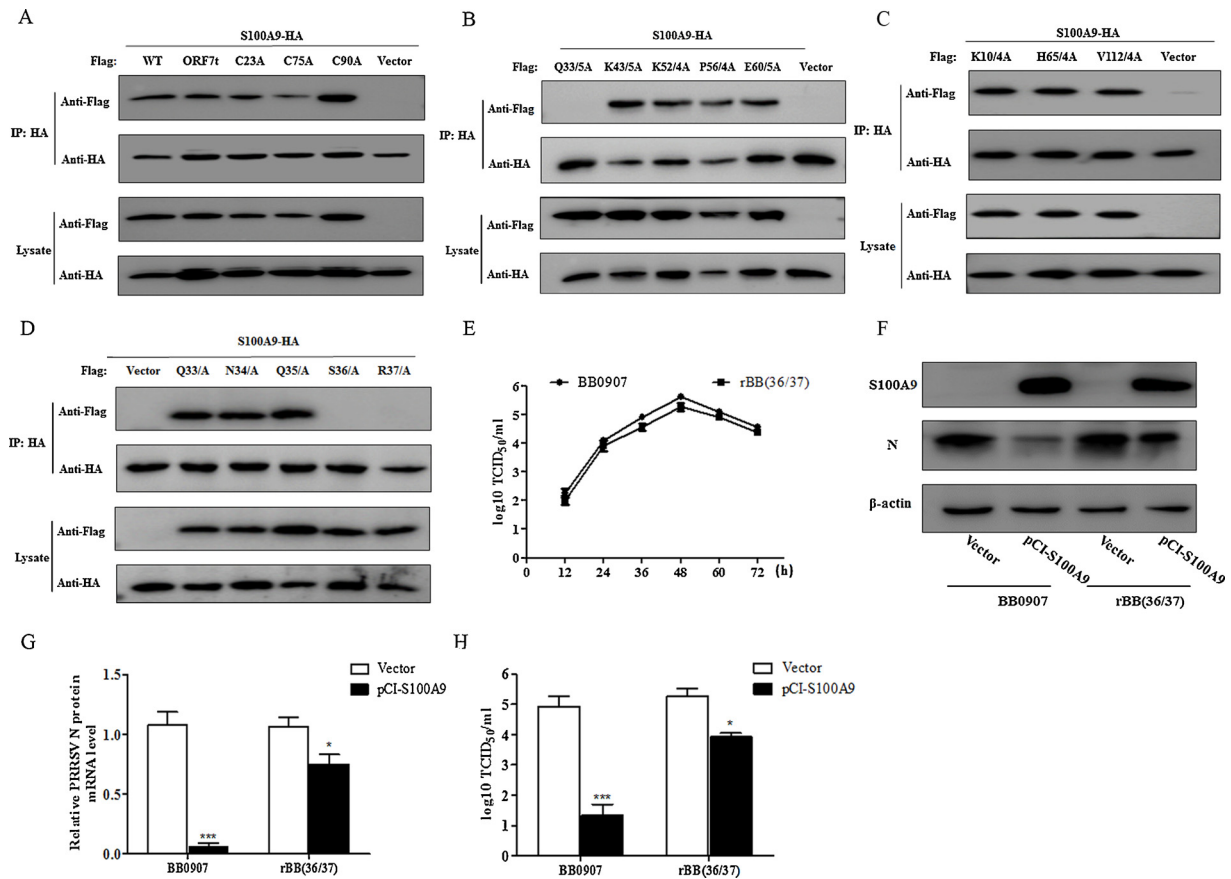
Fig. 5. The key region of the PRRSV N protein necessary for the interaction with S100A9. (A–D) HEK293 T cells co-transfected for 30 h with pCI-S100A9-HA and pCI-*N*-FLAG or the pCI-N*-FLAG series of plasmids, the proteins were immunoprecipitated by an anti-FLAG antibody. Whole cell lysates and IP complexes were analyzed by western blot using anti-FLAG and HA antibodies. (E) The growth kinetics of the wild type PRRSV BB0907 strain and recombinant PRRSV rBB(36/37). (F–H) Marc-145 cells transfected with pCI-S100A9-HA or empty vector followed by an incubation with 0.01 MOI of BB0907 or rBB(36/37). A western blot (F), qPCR (G), and TCID$_{50}$ assay (H) were used to determine the level of viral replication. The data are expressed as the means + standard deviations from three independent experiments.

important role in the regulation of PRRSV replication.

4. Discussion

PRRSV displays a high degree of genetic and antigenic heterogeneity, which poses a continuous challenge for disease control and results in tremendous economic losses to pork producers throughout the world (Tian et al., 2007; Zhang et al., 2016). Although commercial vaccines are available, they provide only limited protection. Pattern recognition receptors (PRRs) play a sentinel role in the activation of the

innate immune system by detecting pathogen associated molecular patterns (PAMPs) associated with viruses and bacteria (Iwasaki and Medzhitov, 2015). PRRs include host restriction factors, many of which are simulated by interferon, which directly or indirectly target multiple stages of the viral life cycle. For instance, the membrane-associated enzyme, cholesterol 25-hydroxylase, inhibits viral entry and degrades viral proteins (Evans et al., 2017; Ke et al., 2017). Moreover, viperin (an IFN-stimulated gene) suppresses HCMV infection by inhibiting viral structural protein synthesis, assembly, and maturation (Chin and Cresswell, 2001). Viperin also destroys lipid rafts, inhibiting the
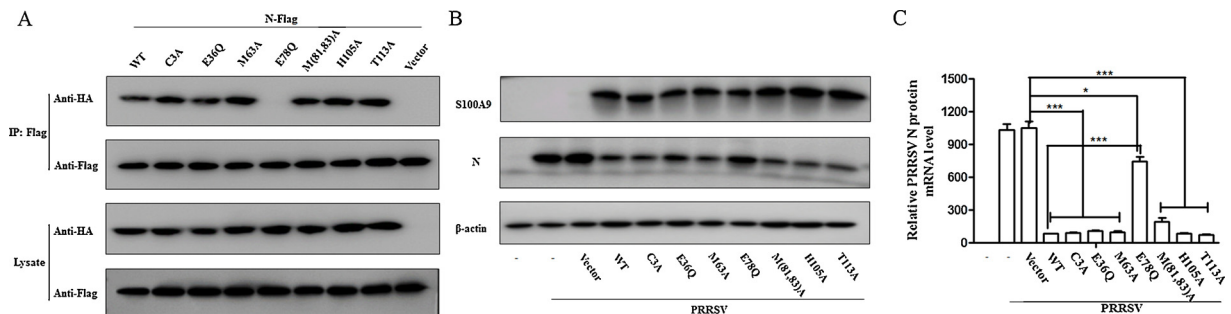

Fig. 6. The key region of S100A9 is necessary for the interaction with PRRSV N protein. (A) Western blot of HEK293T cells co-transfected with plasmids expressing pCI-S100A9 or pCI-S100A9(E78Q) and pCI-*N*-FLAG or empty vector for 30 h. The proteins were immunoprecipitated by an anti-HA antibody. The whole cell lysates and IP complexes were analyzed with an anti-FLAG or HA antibody. (B and C) Marc-145 cells transfected with plasmids expressing mutants of S100A9 for 24 h, then infected with 0.01 MOI of the PRRSV BB0907 strain for 36 h. Viral replication was analyzed by western blot and qPCR. The data are expressed as the means + standard deviations from three independent experiments.
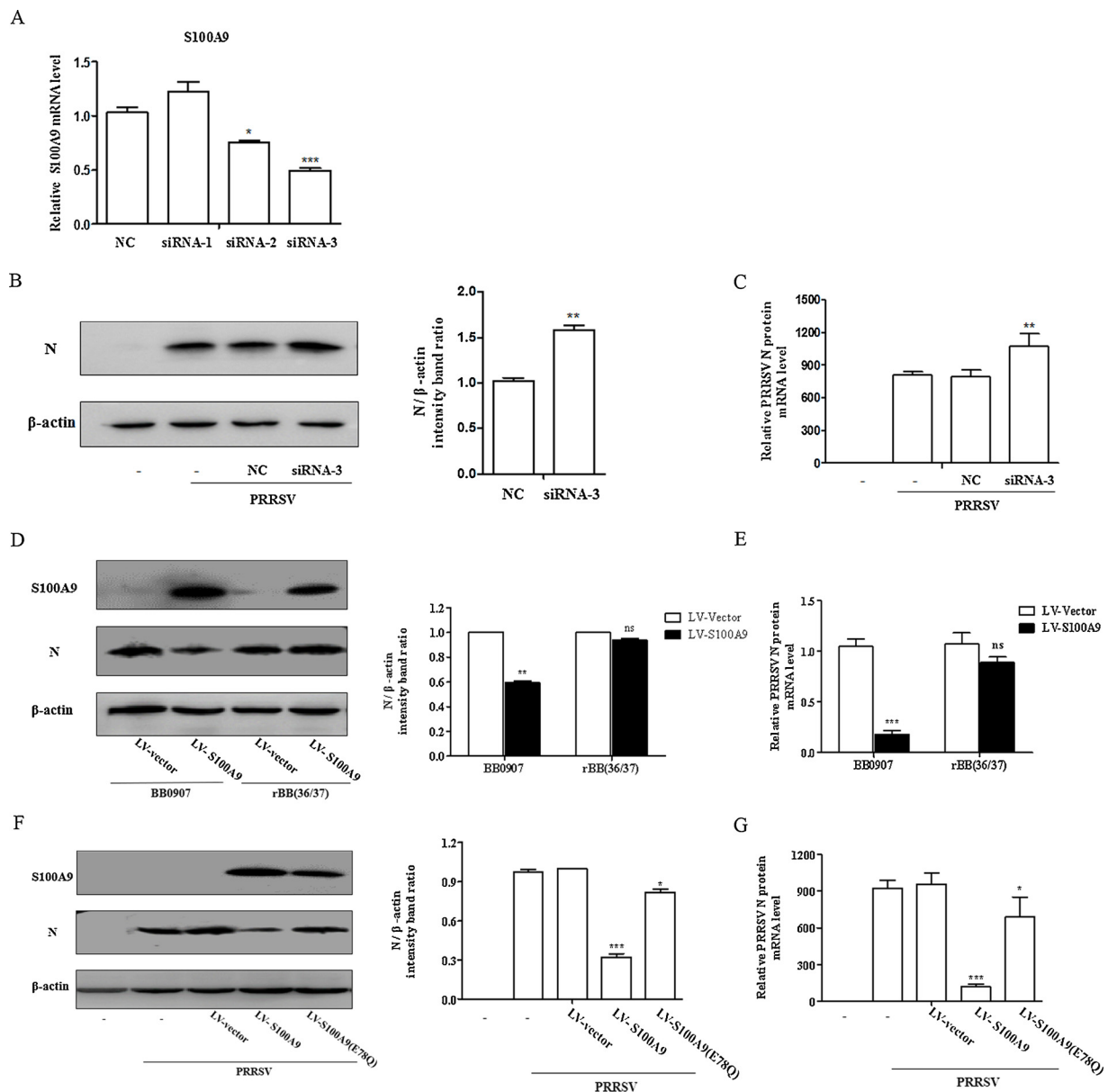
Fig. 7. S100A9 inhibits PRRSV replication in PAMs. (A) The qRT-PCR of PAMs transfected with siRNA targeting porcine *S100A9* or non-specific siRNA. (B and C) Viral replication in PAMs transfected with siRNA-3 or non-specific siRNA for 24 h then infected with 0.01 MOI of PRRSV BB0907, measured by western blot and qPCR. (D–G) Viral replication in PAMs transduced with a lentivirus expressing S100A9 or S100A9(E78Q), (LV-S100A9 and LV-S100A9(E78Q)) and an empty vector (LV-vector). The cells were then infected with 0.01 MOI of PRRSV BB0907 or rBB(36/37), and expression was measured by Western blot and qRT-PCR. The data are expressed as the means + standard deviations from three independent experiments.

budding and release of influenza virus (Wang et al., 2007). TRIM family proteins also interfere at multiple stages of the viral life cycle, including degrading viral proteins (Fan et al., 2016), decreasing gene expression and impeding viral assembly (Barr et al., 2008; Wu et al., 2006); however, as an immunosuppressive virus, PRRSV can negatively regulate the host immune response to promote viral propagation via several pathways, including multiple interferon-pathway suppression (Kim et al., 2010; Beura et al., 2010; Li et al., 2010), host antiviral protein degradation (Huang et al., 2016, 2014), disturbance of monocyte/macrophages, B cell, and T cell development (Huang et al., 2015; Loving et al., 2015; Fan et al., 2015), and reduced expression of antigen presenting molecules (Chen et al., 2018). In the present study, we found that HP-PRRSV infection promoted S100A9 expression in both PAMs and Marc-145 cells. The overexpression and knockdown of S100A9 demonstrated that S100A9 has significant antiviral activity against PRRSV infection. Moreover, the antiviral activity of S100A9 depended on the presence of cellular calcium.

The PRRSV N protein is a vital structural protein required for viral replication. Our previous reports revealed that the viral N protein is associated with the production of CD83 (Chen et al., 2017a, b), Treg cells (Fan et al., 2015), and IL-10 (Liu et al., 2015b), which play an important role in virus-induced immunosuppression. A study by Zhao et al., found that the PRRSV N protein could decrease the antiviral activity of TRIM25 by interfering with TRIM25-mediated RIG-I ubiquitination (Zhao et al., 2019). In the present study, to identify viral proteins that interact with S100A9 and the functional sites of such interactions, we constructed a series of plasmids expressing PRRSV proteins. Co-IP assays showed only the viral N protein was immunoprecipitated by S100A9, and amino acids 36–37 of the N protein were necessary and sufficient for the interaction. Furthermore, recombinant PRRSV rBB(36/37) with the mutations S36A and R37A in the N protein was constructed. It was confirmed that 36–37 aa of the

viral N protein represented the key region at which the viral N protein interacted with S100A9.

DAMPs are host-derived molecules that serve to initiate and perpetuate the innate immune response. The calcium-binding protein, S100A9, belongs to the S100 protein family, and functions as a DAMP. Generally, S100A9 binds to its respective receptor, including RAGE, TLR2, and TLR4, to activate NF-κB or the MAPK signaling pathways (Kwon et al., 2013; Pandolfi et al., 2016). A recent study revealed that some DAMPs are also involved in the regulation of PRRSV replication. For example, HP-PRRSV infection promotes S100A6 expression in PAMs, which is related to the activity of NF-κB activation by HP-PRRSV (Zhou et al., 2015). Additionally, the inhibition of endogenous HSP70 and HSP90 can attenuate PRRSV replication (Dong et al., 2016; Gao et al., 2014); however, there are few reports investigating the role of S100A9 in viral infection. Some previous studies indicate that S100A9 could be induced by poly I:C stimulation (Voss et al., 2012), and human papillomavirus infection also increases S100A9 production (Tugizov et al., 2005). Similarly, the level of S100A9 in patients infected with coronavirus was also upregulated by more than 60-fold (Reghunathan et al., 2005). Because S100A9 is a part of several important immune pathways, it becomes the logical target for viral proteins to interfere with host defense mechanisms. To identify the key region by which S100A9 interacts with the viral N protein, we constructed a series of plasmids expressing S100A9 mutants. The results showed that only the mutant E78Q did not co-precipitate with the N protein and had significantly less antiviral activity compared to the wild type S100A9. Moreover, similar results were also obtained in experiments with PAMs using the recombinant lentiviruses, LV-S100A9 and LV-S100A9(E78Q). These results demonstrated that the E78Q mutation caused a significant decrease in the antiviral activity of S100A9. Moreover, E78 is an S100A9 amino acid necessary for its anti-PRRSV activity.

In summary, we found that S100A9 exhibited prominent anti-PRRSV activity that was dependent on the level of cellular Ca^{2+}. S100A9 inhibits PRRSV replication by interacting with the PRRSV N protein. In addition, E78 in S100A9 played an important role in the regulation of PRRSV replication. These findings provide insight into the host defense mechanisms mediated against PRRSV infection, which should be useful for developing strategies for the control of PRRSV infection.

Acknowledgments

Appendix A. Supplementary data

Supplementary material related to this article can be found, in the online version, at doi:https://doi.org/10.1016/j.vetmic.2019.108498.

References

Barr, S.D., Smiley, J.R., Bushman, F.D., 2008. The interferon response inhibits HIV particle production by induction of TRIM22. PLoS Pathog. 4, e1000007.

Beura, L.K., Sarkar, S.N., Kwon, B., Subramaniam, S., Jones, C., Pattnaik, A.K., Osorio, F.A., 2010. Porcine reproductive and respiratory syndrome virus nonstructural protein 1beta modulates host innate immune response by antagonizing IRF3 activation. J. Virol. 84, 1574–1584.

Burkard, C., Opriessnig, T., Mileham, A.J., Stadejek, T., Ait-Ali, T., Lillico, S.G., Whitelaw, C., Archibald, A.L., 2018. Pigs lacking the scavenger receptor cysteine-rich domain 5 of CD163 are resistant to porcine reproductive and respiratory syndrome virus 1 infection. J. Virol. 92.

Chen, N., Liu, Q., Qiao, M., Deng, X., Chen, X., Sun, M., 2017a. Whole genome characterization of a novel porcine reproductive and respiratory syndrome virus 1 isolate: genetic evidence for recombination between Amervac vaccine and circulating strains in mainland China. Infect. Genet. Evol. 54, 308–313.

Chen, X., Bai, J., Liu, X., Song, Z., Zhang, Q., Wang, X., Jiang, P., 2018. Nsp1alpha of porcine reproductive and respiratory syndrome virus strain BB0907 impairs the function of monocyte-derived dendritic cells via the release of soluble CD83. J. Virol. 92.

Chen, X., Zhang, Q., Bai, J., Zhao, Y., Wang, X., Wang, H., Jiang, P., 2017b. The nucleocapsid protein and nonstructural protein 10 of highly pathogenic porcine reproductive and respiratory syndrome virus enhance CD83 production via NF-kappaB and Sp1 signaling pathways. J. Virol. 91.

Chin, K.C., Cresswell, P., 2001. Viperin (cig5), an IFN-inducible antiviral protein directly induced by human cytomegalovirus. Proc. Natl. Acad. Sci. U. S. A. 98, 15125–15130.

Darweesh, M.F., Rajput, M., Braun, L.J., Rohila, J.S., Chase, C., 2018. BVDV Npro protein mediates the BVDV induced immunosuppression through interaction with cellular S100A9 protein. Microb. Pathog. 121, 341–349.

Dong, S., Liu, L., Wu, W., Armstrong, S.D., Xia, D., Nan, H., Hiscox, J.A., Chen, H., 2016. Determination of the interactome of non-structural protein12 from highly pathogenic porcine reproductive and respiratory syndrome virus with host cellular proteins using high throughput proteomics and identification of HSP70 as a cellular factor for virus replication. J. Proteomics 146, 58–69.

Evans, A.B., Dong, P., Loyd, H., Zhang, J., Kraus, G.A., Carpenter, S., 2017. Identification and characterization of small molecule inhibitors of porcine reproductive and respiratory syndrome virus. Antiviral Res. 146, 28–35.

Fan, B., Liu, X., Bai, J., Li, Y., Zhang, Q., Jiang, P., 2015. The 15N and 46R residues of highly pathogenic porcine reproductive and respiratory syndrome virus nucleocapsid protein enhance regulatory t lymphocytes proliferation. PLoS One 10, e138772.

Fan, W., Wu, M., Qian, S., Zhou, Y., Chen, H., Li, X., Qian, P., 2016. TRIM52 inhibits Japanese encephalitis virus replication by degrading the viral NS2A. Sci. Rep. 6, 33698.

Gao, J., Xiao, S., Liu, X., Wang, L., Zhang, X., Ji, Q., Wang, Y., Mo, D., Chen, Y., 2014. Inhibition of HSP90 attenuates porcine reproductive and respiratory syndrome virus production in vitro. Virol. J. 11, 17.

Huang, C., Du, Y., Yu, Z., Zhang, Q., Liu, Y., Tang, J., Shi, J., Feng, W.H., 2016. Highly pathogenic porcine reproductive and respiratory syndrome virus Nsp4 cleaves VISA to impair antiviral responses mediated by RIG-I-like receptors. Sci. Rep. 6, 28497.

Huang, C., Zhang, Q., Feng, W.H., 2015. Regulation and evasion of antiviral immune responses by porcine reproductive and respiratory syndrome virus. Virus Res. 202, 101–111.

Huang, C., Zhang, Q., Guo, X.K., Yu, Z.B., Xu, A.T., Tang, J., Feng, W.H., 2014. Porcine reproductive and respiratory syndrome virus nonstructural protein 4 antagonizes beta interferon expression by targeting the NF-kappaB essential modulator. J. Virol. 88, 10934–10945.

Iwasaki, A., Medzhitov, R., 2015. Control of adaptive immunity by the innate immune system. Nat. Immunol. 16, 343–353.

Jiang, P., Chen, P.Y., Dong, Y.Y., Cai, J.L., Cai, B.X., Jiang, Z.H., 2000. Isolation and genome characterization of porcine reproductive and respiratory syndrome virus in P.R. China. J. Vet. Diagn. Invest. 12, 156–158.

Jing, H., Tao, R., Dong, N., Cao, S., Sun, Y., Ke, W., Li, Y., Wang, J., Zhang, Y., Huang, H., Dong, W., 2019. Nuclear localization signal in TRIM22 is essential for inhibition of type 2 porcine reproductive and respiratory syndrome virus replication in MARC-145 cells. Virus Genes 55, 660–672.

Ke, W., Fang, L., Jing, H., Tao, R., Wang, T., Li, Y., Long, S., Wang, D., Xiao, S., 2017. Cholesterol 25-hydroxylase inhibits porcine reproductive and respiratory syndrome virus replication through enzyme activity-dependent and -Independent mechanisms. J. Virol. 91.

Kim, O., Sun, Y., Lai, F.W., Song, C., Yoo, D., 2010. Modulation of type I interferon induction by porcine reproductive and respiratory syndrome virus and degradation of CREB-binding protein by non-structural protein 1 in MARC-145 and HeLa cells. Virology 402, 315–326.

Kwon, C.H., Moon, H.J., Park, H.J., Choi, J.H., Park, D.Y., 2013. S100A8 and S100A9 promotes invasion and migration through p38 mitogen-activated protein kinase-dependent NF-kappaB activation in gastric cancer cells. Mol. Cells 35, 226–234.

Li, C., Zhuang, J., Wang, J., Han, L., Sun, Z., Xiao, Y., Ji, G., Li, Y., Tan, F., Li, X., Tian, K., 2016. Outbreak investigation of NADC30-Like PRRSV in South-East China. Transbound. Emerg. Dis. 63, 474–479.

Li, H., Zheng, Z., Zhou, P., Zhang, B., Shi, Z., Hu, Q., Wang, H., 2010. The cysteine protease domain of porcine reproductive and respiratory syndrome virus non-structural protein 2 antagonizes interferon regulatory factor 3 activation. J. Gen. Virol. 91, 2947–2958.

Li, Y., Wang, X., Bo, K., Wang, X., Tang, B., Yang, B., Jiang, W., Jiang, P., 2007. Emergence of a highly pathogenic porcine reproductive and respiratory syndrome virus in the Mid-Eastern region of China. Vet. J. 174, 577–584.

Liu, J., Bai, J., Zhang, J., Jiang, Z., Wang, X., Li, Y., Jiang, P., 2013. Hsp70 positively regulates porcine circovirus type 2 replication in vitro. VIROLOGY 447, 52–62.

Liu, J., Zhang, X., Ma, C., You, J., Dong, M., Yun, S., Jiang, P., 2016. Heat shock protein 90 is essential for replication of porcine circovirus type 2 in PK-15 cells. Virus Res. 224, 29–37.

Liu, X., Fan, B., Bai, J., Wang, H., Li, Y., Jiang, P., 2015a. The N-N non-covalent domain of the nucleocapsid protein of type 2 porcine reproductive and respiratory syndrome virus enhances induction of IL-10 expression. J. Gen. Virol. 96, 1276–1286.

Liu, X., Fan, B., Bai, J., Wang, H., Li, Y., Jiang, P., 2015b. The N-N non-covalent domain of the nucleocapsid protein of type 2 porcine reproductive and respiratory syndrome virus enhances induction of IL-10 expression. J. Gen. Virol. 96, 1276–1286.

Loving, C.L., Osorio, F.A., Murtaugh, M.P., Zuckermann, F.A., 2015. Innate and adaptive immunity against porcine reproductive and respiratory syndrome virus. Vet. Immunol. Immunopathol. 167, 1–14.

Pandolfi, F., Altamura, S., Frosali, S., Conti, P., 2016. Key role of DAMP in inflammation, cancer, and tissue repair. Clin. Ther. 38, 1017–1028.

Pouwels, S.D., Heijink, I.H., Ten, H.N., Vandenabeele, P., Krysko, D.V., Nawijn, M.C., van Oosterhout, A.J., 2014. DAMPs activating innate and adaptive immune responses in COPD. Mucosal Immunol. 7, 215–226.

Reghunathan, R., Jayapal, M., Hsu, L.Y., Chng, H.H., Tai, D., Leung, B.P., Melendez, A.J., 2005. Expression profile of immune response genes in patients with severe acute respiratory syndrome. BMC Immunol. 6, 2.

Tian, K., Yu, X., Zhao, T., Feng, Y., Cao, Z., Wang, C., Hu, Y., Chen, X., Hu, D., Tian, X., Liu, D., Zhang, S., Deng, X., Ding, Y., Yang, L., Zhang, Y., Xiao, H., Qiao, M., Wang, B., Hou, L., Wang, X., Yang, X., Kang, L., Sun, M., Jin, P., Wang, S., Kitamura, Y., Yan, J., Gao, G.F., 2007. Emergence of fatal PRRSV variants: unparalleled outbreaks of atypical PRRS in China and molecular dissection of the unique hallmark. PLoS One 2, e526.

Trinh, Q.D., Pham, N.T., Fuwa, K., Takada, K., Komine-Aizawa, S., Honda, M., Ushijima, H., Hayakawa, S., 2016. High mobility group Box 1 protein enhances HIV replication in newly infected primary t cells. Clin. Lab. 62, 2305–2311.

Tugizov, S., Berline, J., Herrera, R., Penaranda, M.E., Nakagawa, M., Palefsky, J., 2005. Inhibition of human papillomavirus type 16 E7 phosphorylation by the S100 MRP-8/14 protein complex. J. Virol. 79, 1099–1112.

Voss, A., Gescher, K., Hensel, A., Nacken, W., Zanker, K.S., Kerkhoff, C., 2012. Double-stranded RNA induces S100 gene expression by a cycloheximide-sensitive factor. FEBS Lett. 586, 196–203.

Wang, C., Zeng, N., Liu, S., Miao, Q., Zhou, L., Ge, X., Han, J., Guo, X., Yang, H., 2017a. Interaction of porcine reproductive and respiratory syndrome virus proteins with SUMO-conjugating enzyme reveals the SUMOylation of nucleocapsid protein. PLoS One 12, e189191.

Wang, L.J., Xie, W., Chen, X.X., Qiao, S., Zhao, M., Gu, Y., Zhao, B.L., Zhang, G., 2017b. Molecular epidemiology of porcine reproductive and respiratory syndrome virus in Central China since 2014: the prevalence of NADC30-like PRRSVs. Microb. Pathog. 109, 20–28.

Wang, X., Hinson, E.R., Cresswell, P., 2007. The interferon-inducible protein viperin inhibits influenza virus release by perturbing lipid rafts. Cell Host Microbe 2, 96–105.

Wu, X., Anderson, J.L., Campbell, E.M., Joseph, A.M., Hope, T.J., 2006. Proteasome inhibitors uncouple rhesus TRIM5alpha restriction of HIV-1 reverse transcription and infection. Proc. Natl. Acad. Sci. U. S. A. 103, 7465–7470.

Wuerth, J.D., Habjan, M., Wulle, J., Superti-Furga, G., Pichlmair, A., Weber, F., 2018. NSs protein of sandfly fever sicilian phlebovirus counteracts interferon (IFN) induction by masking the DNA-Binding domain of IFN regulatory factor 3. J. Virol. 92.

Zhang, Q., Jiang, P., Song, Z., Lv, L., Li, L., Bai, J., 2016. Pathogenicity and antigenicity of a novel NADC30-like strain of porcine reproductive and respiratory syndrome virus emerged in China. Vet. Microbiol. 197, 93–101.

Zhao, K., Li, L.W., Jiang, Y.F., Gao, F., Zhang, Y.J., Zhao, W.Y., Li, G.X., Yu, L.X., Zhou, Y.J., Tong, G.Z., 2019. Nucleocapsid protein of porcine reproductive and respiratory syndrome virus antagonizes the antiviral activity of TRIM25 by interfering with TRIM25-mediated RIG-I ubiquitination. Vet. Microbiol. 233, 140–146.

Zhao, K., Li, L.W., Zhang, Y.J., Jiang, Y.F., Gao, F., Li, G.X., Yu, L.X., Zhao, W.Y., Shan, T.L., Zhou, Y.J., Tong, G.Z., 2018. MOV10 inhibits replication of porcine reproductive and respiratory syndrome virus by retaining viral nucleocapsid protein in the cytoplasm of Marc-145cells. Biochem. Biophys. Res. Commun. 504, 157–163.

Zhou, X., Wang, P., Michal, J.J., Wang, Y., Zhao, J., Jiang, Z., Liu, B., 2015. Molecular characterization of the porcine S100A6 gene and analysis of its expression in pigs infected with highly pathogenic porcine reproductive and respiratory syndrome virus (HP-PRRSV). J. Appl. Genet. 56, 355–363.